Blood Makes a Difference: Experimental Evaluation of Molecular Communication in Different Fluids

Lisa Y. Debus, *Student Member, IEEE*, Mario J. Wilhelm, Henri Wolff, Luiz C. P. Wille, *Student Member, IEEE*, Tim Rese, Michael Lommel, Jens Kirchner, *Senior Member, IEEE* and Falko Dressler, *Fellow, IEEE*

***Abstract*—The experimental appraisal of existing molecular communication (MC) testbeds and modeling frameworks in real blood is an important step for future internet of bio-nano things applications. In this paper, we experimentally compare the MC flow characteristics of water, blood substitute, and real porcine blood for a previously presented superparamagnetic iron oxide nanoparticles (SPION) MC testbed. We perform an extensive analysis of the channel impulse response (CIR) behavior of the testbed for the different fluids. Based on the identified MC flow characteristics, we extend an existing mathematical framework for our SPION testbed to capture the flow properties of blood. We evaluate its applicability to the collected data in comparison to two existing theoretical CIR models for MC in blood. In our work, we see that the added complexity of the transmission in blood opens up promising new possibilities to improve communication through the human circulatory system.**

***Index Terms*—Molecular Communications, Fluid-based Communication, Nanoparticles, In-body Communication, Testbeds**

I. Introduction

Molecular communication (MC) was proposed as an enabler for communication through the human body via the human circulatory system (HCS). Akyildiz et al. [1] coined the term internet of bio-nano things (IoBNT) to describe the concept of biocompatible nanomachines cooperating in the HCS. Their vision used MC to facilitate communication between the nanomachines. To this day, this concept promises to make continuous disease monitoring and precision medicine a reality. Multiple steps have been taken to make MC a viable solution in the life sciences. Many testbeds employing different signaling molecules were developed [2], [3], their theoretical and practical performance was evaluated [4], [5], and based on these systems, different problems, such as modulation, coding, or synchronization [6]–[9], were tackled. Although these solutions are valuable and address many important questions for the future use of MC in the human body, they leave one important question open. Most of the existing research assumes a flow medium that behaves like water or, in the case of the testbeds, actually is water. In the HCS, though, the flow medium is not a simple Newtonian fluid, but instead blood, a complex 2-phase non-Newtonian fluid.

The difference between the two media leads, for example, to a different flow profile [10] and changed particle distribution [11]. While using simpler systems with water is an option for first evaluations and proof-of-concept analysis, it is not sufficient for the move from theory to the real world. If we want to transfer MC to medical in-body applications in the HCS, we must understand how we can model and work with the movement of MC signaling particles through blood and the human body. Huang et al. [10] and Yue et al. [12] recently approached the changes introduced by the medium change by evaluating the channel impulse response (CIR) in blood theoretically. To produce mathematical models grounded in reality, we must approach the topic not only from a theoretical perspective but also from an experimental perspective.

In this work, we will for the first time experimentally appraise the applicability of existing CIR models to MC transmission in blood by comparing them to measurements of MC in different media. For our experiments, we deploy the superparamagnetic iron oxide nanoparticles (SPION) testbed developed by Bartunik et al. [13] in a simple setup inspired by the Arteria radialis. We evaluate the behavior of the system for water, blood substitute, and porcine blood, with four different channel lengths, two different transmitter (Tx) geometries, and two different flow velocities. Using the collected data, we compare the existing mathematical model to the observed behavior and adapt the model to the presented setup. This presents an important first step for the transfer of simplified theoretical models to more complex real-world behavior and the inclusion of MC in future medical applications.

Our key contributions can be summarized as follows:

- We experimentally compared the MC flow characteristics of water, blood substitute, and real porcine blood.
- We extended a mathematical framework to cover the identified MC flow characteristics to capture the flow properties of blood.

II. Experiment Setup

In the following, we will explain the setup, the signaling particles, and the background flow media.

Lisa Y. Debus and Falko Dressler are with the School for Electrical Engineering and Computer Science, Technische Universität Berlin, Berlin, Germany, email: {debus, dressler}@ccs-labs.org

Mario J. Wilhelm, Henri Wolff, Tim Rese, and Michael Lommel are with the Deutsches Herzzentrum der Charité, Institute of Computer-assisted Cardiovascular Medicine, Biofluid Mechanics Laboratory, Berlin, Germany and Charité – Universitätsmedizin Berlin, corporate member of Freie Universität Berlin and Humboldt-Universität zu Berlin, Berlin, Germany, email: {mario.wilhelm, tim.rese, henri.wolff, michael.lommel}@charite.de

Luiz C. P. Wille and Jens Kirchner are with the Institute for Electronics Engineering, Friedrich-Alexander-Universität Erlangen-Nürnberg (FAU), Erlangen, Germany, email: {luiz.wille, jens.kirchner}@fau.de

Jens Kirchner is also with Fachhochschule Dortmund, University of Applied Sciences and Arts, Dortmund, Germany.

This work was supported in part by the project IoBNT funded by the German Federal Ministry of Research, Technology and Space (BMFTR) under grant number 16KIS1986K, by the project NaBoCom funded by the German Research Foundation (DFG) under grant number DR 639/21-2, and by the project SyMoCADS funded by the German Research Foundation (DFG) under grant number GRK 2950, Project-ID 509922606.

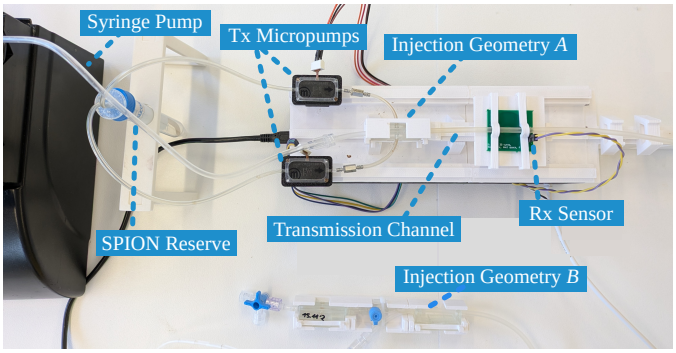

Fig. 1. The setup of the testbed for the evaluation with different fluids with both injection geometries.

A. Testbed Setup

For our experiments, we use the SPION-based MC testbed introduced by Bartunik et al. [13] as shown in Fig. 1. The testbed consists of a syringe pump, a Tx with two micropumps, an MC channel of varying length, a receiver (Rx) with two sensors, and a waste container. The syringe pump provides the background flow for all experiments. The medium flows through silicone tubing along the Tx and the Rx into the waste container. The radius, $r = 1.5\,\mathrm{mm}$, and the maximum length, $d_{\max} = 20\,\mathrm{cm}$, of the channel are set according to the approximate dimensions of the Arteria radialis [14]. The maximum flow velocity is set according to the average expected blood flow velocity in the Arteria radialis with $v_{\max} = 15\,\mathrm{cm/s}$ [15].

The following two Tx geometries were used: In geometry A, we inject with two micropumps from opposite sides of the channel tubing to achieve an approximately uniform injection geometry. In geometry B, we inject via a cannula into the center of the bloodstream. In both cases, we inject the same volume of SPIONs at a flow rate of 10 mL/min and use valves to stop backflow and leakage. For the Rx, we employ two identical planar sensor coils [16] set next to each other.[1] The emitted SPIONs influence the inductivity of the coil when they flow along it in the channel. We observe the change in inductivity by measuring the resonance frequency of the coils and describe it with the resonance frequency shift. This shift changes according to the change in the external magnetic field, e.g., the number of magnetic particles and their speed.

B. Signaling Particles

The testbed uses superparamagnetic iron oxide nanoparticles (SPION) particles for signaling. They were synthesized using co-precipitation by the Section for Experimental Oncology and Nanomedicine (SEON) of the University Hospital Erlangen [17]. The SPION particles consist of a magnetite core that is surrounded by a coating that makes the particle compatible with the fluid it is used in. The coating substance is lauric acid (LA) for water. For use in blood, the LA layer is substituted by dopamine and binds a layer of human serum albumin. They have a hydrodynamic diameter of approximately $50\,\mathrm{nm}$ [13]. In all experiments, we use a SPION solution with an iron concentration of $6\,\mathrm{mg/mL}$ diluted in distilled water.

[1]The program used for the control of the Tx and Rx is available online at https://github.com/LCPW/UnifiedGUI

TABLE I
EVALUATED CONFIGURATIONS

Parameter	Values
background flow medium	water, blood substitute (water-glycerin), porcine blood
channel length	5, 10, 15 and 20 cm from the injection to the middle of the sensor coil
background flow velocity	7.5 and 15 cm/s
injection geometry	90° from the side of the channel, via a cannula directly into a channel at 0°

C. Background Flow Medium

In our experiments, we use three different fluids for the background flow. As a baseline and an example of a Newtonian fluid, we use distilled water at 20° and as a substitute for human blood and an example of a non-Newtonian two-phase fluid, we use porcine blood at $38\,^{\circ}\mathrm{C}$. The blood had a hematocrit of 40.2% and was sourced from a local butchery from a single pig and used for the experiments at the same day as the slaughter. To stop coagulation, the blood was heparinized with $0.108\,\mathrm{g}$ heparin per litre blood.

To evaluate the impact of viscosity, we additionally evaluate a water-glycerin mixture as blood substitute. With a mixing ratio of one part glycerin to two parts water, we adjust its viscosity at $20\,^{\circ}\mathrm{C}$ to equal the viscosity of the used blood [18].

III. Experiment Results

We first comparatively evaluate the collected experimental data for different fluids and then consider the injection geometries and background flow velocities.[2] The studied configurations of the setup are summarized in Table I.

A. Background Flow Medium

Fig. 2 shows the sensor response at the Rx for blood, blood substitute, and water at a distance of $d = 5\,\mathrm{cm}$ and $d = 15\,\mathrm{cm}$ over time. The measurements show the importance of the fluid viscosity for the CIR. While the peak frequency shifts for blood and blood substitute are around the same level, the values in water are consistently lower. Here, the lower viscosity leads to the emitted signal spreading wider faster.

We additionally observe an important property for the results in blood. While the CIR in blood substitute and water only shows one peak, the CIR in blood shows two. This is due to the short increase in the volumetric flow rate produced by the injection. The sensor coils detect the pulse moving through the channel via the iron contained in the blood and record the signal overlapping with the signal produced by the SPIONs. The reaction of the sensor coil to the iron content in the blood is also visible in a constant resonance frequency offset produced by the blood moving along the Rx.

B. Flow Velocity

The CIR of the three fluids for $v_{\max} = 7.5$ and $15\,\mathrm{cm/s}$ is shown in Fig. 3. In the results, we observe the peaks

[2]The collected data set and a supplementary visual summary of the same are available online via Zenodo under https://doi.org/10.5281/zenodo.15064515.

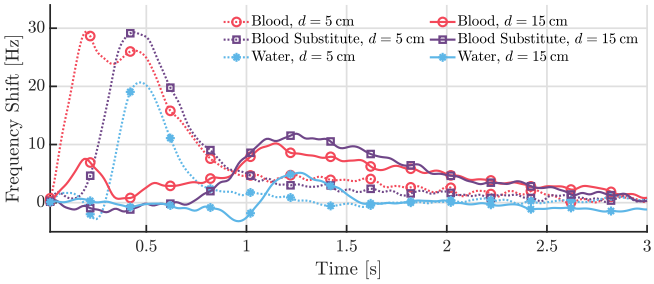

Fig. 2. CIR in blood, blood substitute, and water averaged over 8 consecutive pulses at a distance of $d = 5$ and $15\,\mathrm{cm}$, flow velocity of $7.5\,\mathrm{cm/s}$ and injected at a 90° angle.

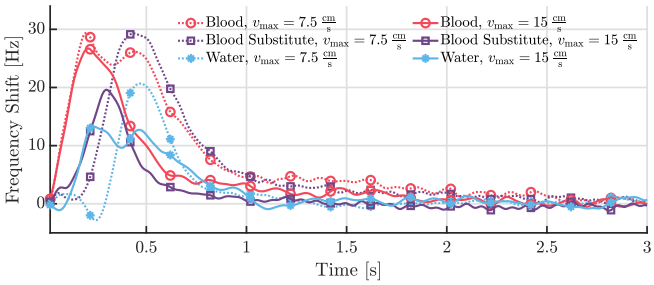

Fig. 3. CIR in blood, blood substitute, and water for a maximum background flow velocity of 7.5 and $15\,\mathrm{cm/s}$ averaged over 8 consecutive pulses at a distance of $d = 5\,\mathrm{cm}$ and injected at a 90° angle.

registering the SPIONs earlier and with a lower amplitude for a higher speed. While for both velocities the timing of the injection peak in blood is approximately the same, we observe a decrease in the amplitude for a higher speed. Here, the difference between the injection speed and the background flow speed is lower, leading to a decrease in amplitude of the injection peak. Additionally, for $v_{\max} = 15\,\mathrm{cm/s}$, the injection peak completely overlaps with the peak produced by the SPIONs. The height of the peak registering the SPIONs changes with the velocity gradient over the radius of the channel. For a higher maximum velocity at the middle of the channel, the velocity gradient towards the channel wall is higher. As a result, the signal spreads wider faster and produces a lower frequency shift.

C. Injection Geometry

Fig. 4 shows the CIR in the different fluids for an injection at 90° from the side of the channel, i.e., injection geometry *A*, and via a cannula directly into a channel at 0°, i.e., injection geometry *B*. The results show the importance of the injection geometry for the observed signal. While the amplitude and timing of the initial injection peak in blood is approximately equal for the evaluated configurations, the peak representing the registered SPIONs varies greatly for all fluids. For injection geometry *B*, we detect the SPIONs slightly later and register a much lower amplitude and wider signal. During our experiments, we observed that the injection through the cannula appears to enhance mixing effects that lead to the signal impulse spreading into unrecognizability much faster. The injection from the side of the channel, on the other side, seems to produce an initial distribution that is more localized at the center of the channel, leading to a peak that is not pulled apart as much. In the measurements in water in 3, on the other hand, we see a physical problem with the injection

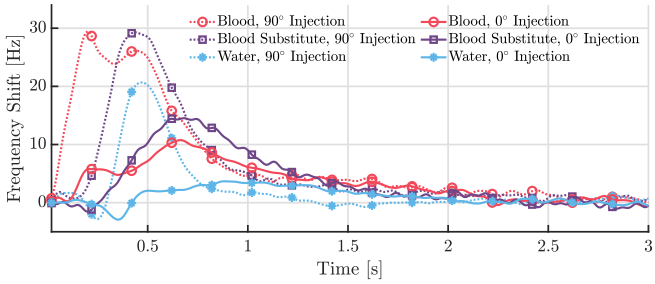

Fig. 4. CIR in blood, blood substitute, and water for an injection at 0° and 90° averaged over 8 consecutive pulses at a distance of $d = 5\,\mathrm{cm}$ and a background flow velocity of $7.5\,\mathrm{cm/s}$.

via two injection points. If the micropumps are not perfectly synchronized, the symbol can split up slightly into two peaks.

IV. Mathematical Model

In the following, we briefly discuss the channel characteristics defining transmission in different fluids, present the proposed model, and compare it to the collected measurements and to two existing CIR models for MC in blood.[3]

A. Channel Characteristics

Fluid flow can be either laminar or turbulent. For our models to work, it is crucial that we work with laminar flow as turbulent flow would introduce more complex behavior. The Reynolds number (Re) can be used to determine which type of flow occurs in the channel. We calculate it as

$$Re = \frac{2r \cdot v_{\text{eff}}}{\nu}, \tag{1}$$

where $2r$ is the channel diameter, v_{eff} the average velocity over a channel cross section, and ν the kinematic viscosity, which is in the range of $10^{-6}\,\mathrm{m^2/s}$ [18], [19] for the used fluids. Using this and the values in Section II-A we calculate

$$v_{\text{eff}} = \frac{v_{\max} \cdot (\alpha + 1)}{3\alpha + 1}, \tag{2}$$

where α is the flow behavior index of the Power-law model and $\alpha_{\text{blood}} = 0.357$ and $\alpha_{\text{blood substitute}} = \alpha_{\text{water}} = 1$, we estimate Re [10]. An Re value below 2100 indicates laminar flow in circular transmission tubes [20]. With $Re \approx 10^2 \ll 2100$ we can safely assume this to be the case in our setting.

B. Mathematical Model

We base our CIR analysis on the model previously presented by Unterweger et al. [19]. We extend their approach to include the parameter α as mentioned above to model the change of the flow profile for non-Newtonian fluids. For Newtonian fluids, i.e., $\alpha = 1$, the model equals the original formula. Based on Unterweger et al. [19] and these considerations, the expected observation probability can be described as:

$$P_{\text{ob}}(t) = \begin{cases} 0 & , \quad t \leq \frac{d}{v_{\max}} \\ 1 - \left(\frac{d}{v_{\max} \cdot t}\right)^s & , \frac{d}{v_{\max}} < t \leq \frac{d+c_z}{v_{\max}} \\ \frac{(d+c_z)^s - d^s}{(v_{\max} \cdot t)^s} & , \frac{d+c_z}{v_{\max}} < t, \end{cases} \tag{3}$$

[3]The Python and MATLAB scripts from our evaluation are available under https://github.com/tkn-tub/Molecular_Communication_in_Blood.

where d is the distance between Rx and Tx, c_z the depth of the Rx along the z axis and $v_{\max}$ the maximum velocity in the channel. The newly introduced shape factor s is calculated as

$$s = \frac{(\beta + 1) \cdot 2\alpha}{\alpha + 1}, \tag{4}$$

where α is the shape factor defined by the fluid viscosity according to the Power-Law model, which is multiplied by $\beta + 1$, the form factor from Unterweger et al. [19] describing the initial distribution of molecules over the channel diameter.

C. Model Evaluation

Fig. 5 shows the development of the CIR in blood over an increasing distance $d = 5,\ 10,\ 15$ and $20\,\mathrm{cm}$ together with the fitted mathematical model. The timing of the initial injection peak stays the same for the evaluated distances, while its amplitude decreases slightly over larger distances. This may be due to the elasticity of the silicone tubing used for the channel, similar to the Windkessel effect in the HCS. The Windkessel effect describes the equalization of the pulsatile ejection of blood by the heart into a continuous and significantly lower-loss flow through the body. This effect is caused by the elasticity of the large arteries, especially the aorta, and can also be generated by elastic tubes or compressible fluids. The amplitude of the peak induced by the SPION transmission, on the other hand, decreases much more with the increasing distance. At the same time, the recorded signal becomes wider as the transmitted signaling molecules spread farther apart.

Together with the collected measurements, we visualize the mathematical model from Eq. (3). It was fitted to the experiment setup by minimizing the mean square error (MSE) between model and measurements. To correctly include the initial injection peak, we used a weighted sum consisting of two P_{ob} equations to represent the CIR. The figure shows that our model can accurately replicate the system behavior.

D. Model Comparison

In Fig. 6, we show our fitted model in comparison with two existing theoretical models for an CIR in blood fitted to our measurement data by minimizing the MSE. While the model by Huang et al. [10] does consider non-Newtonian flow behavior in the flow profile, it only uses the profile's average velocity in the calculations. This simplification leads to the formula not accurately representing the pulling apart of the injected particle cloud due to the velocity gradient along the radius. For the peak directly after the injection, the problem is not visible in the results, yet. In the peak representing the SPION, which takes longer to reach the receiver, we see the influence of the use of a single velocity in the calculations. The model peak occurs later and in the middle of a symmetric CIR curve in comparison to the real measurements that show a quick increase in the frequency shift followed by a longer tail. The model by Yue et al. [12] shows a similarly delayed peak. With a corrected peak position, this simpler model could potentially be helpful for estimating the arrival of the bulk of the particles. For a more elaborate analysis, though, we face the problem that the model does not accurately represent the overall shape of the measurements. Overall, we see that our model currently matches the collected measurements best.

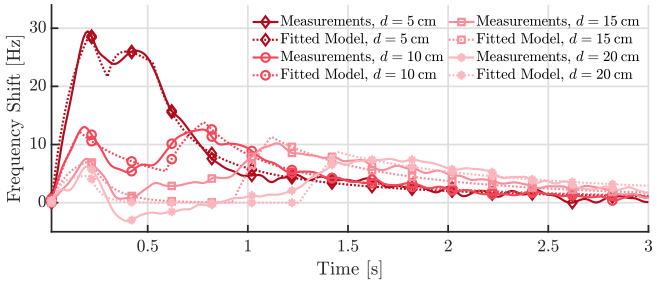

Fig. 5. CIR in blood averaged over 8 consecutive pulses for a flow velocity of $7.5\,\mathrm{cm/s}$ and injection at a 90° angle with fit according to Eq. (3) for different communication distances over time.

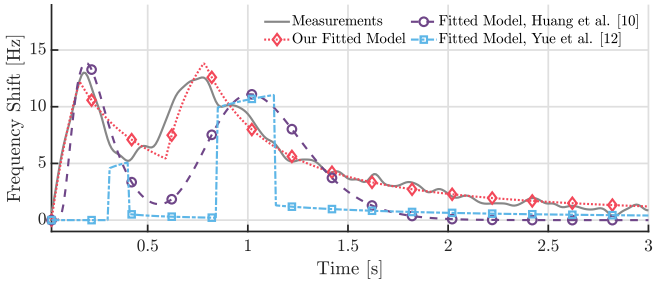

Fig. 6. CIR in blood averaged over 8 consecutive pulses at a distance of $d = 10\,\mathrm{cm}$ with a flow velocity of $7.5\,\mathrm{cm/s}$ and injection at a 90° angle with the fitted mathematical models in Eq. (3), [10], and [12] over time.

V. Discussion

The presented results show the importance of modeling molecular communication (MC) in blood rather than water or blood substitute. If MC is supposed to enable future IoBNT applications, its behavior in this environment must be well known. While the blood-based channel may introduce negative effects at some points, our results show that it can also introduce CIR characteristics that open new possibilities.

The initial peak induced by the increase in volumetric flow rate from the injection has a similar amplitude, width, and timing over all evaluated distances. With its reliable behavior, it could potentially be useful for localization and identification of communication participants. Especially in more complex networks with bifurcations, the added information from the injection peak might offer huge advantages. The evaluation of the testbed in more complex networks with different bifurcations is therefore an important step for future research.

Additionally, we see in our results that the decision of how signaling molecules are brought into the system makes a big difference for the observed CIR. While an exact injection at a 90° angle is unlikely for medical applications in the human body, it is essential that we consider alternative options for future testbeds. Here, our results for the different background flow velocities show a possible approach to mitigating the disadvantages introduced by a given injection method. If the distance between Tx and Rx is known, the combination of an adjustment of the velocity of the particles and the option to overlap the initial injection peak and the one from the SPIONs might improve the quality of the transmitted signal.

We must accept that the evaluation of MC testbeds with blood will not be possible in all laboratory setups. It is

therefore important that we, on the one hand, find appropriate alternatives that replicate the behavior of blood in the MC testbed and, on the other hand, find appropriate mathematical models that describe the same. For the used SPION testbed, that means that an appropriate substitute must not only replicate the fluid dynamics of blood but also its influence on the observed inductivity of the sensor coil. To accurately replicate the particle flow through the HCS, we must comparatively evaluate the behavior of human and porcine blood. Additionally, the influence of different blood characteristics on the particle flow behavior must be evaluated. In future work, we will endeavor to extend our mathematical model to include these physical parameters to enable further theoretical analysis of the communication performance of the testbed.

Our current testbed setup enables a first look at particle flow behavior in blood from an MC standpoint. To produce comparable results, we used the same simple setup and blood from one single animal for all measurements. This also means that we only evaluated a single configuration of tubing and blood. While we already address the necessity to evaluate human blood in comparison to porcine blood and to evaluate different blood characteristics above, we must also not forget to extend our testbed setup. This means adapting the tubing and pumping equipment for different scenarios. Since the shown model is driven by a continuous volume flow of blood and blood substitute, effects such as the Windkessel effect do not come into play based on the background flow. Characteristics such as a realistic elasticity of the silicon tubes will have to be taken into account for future models with a pulsatile flow, though. Evaluating the particle flow behavior and sensing capabilities of our testbed in pulsatile flow is a requirement for a move to in vivo or clinical testing. While we are currently still very far away from that move, we must endeavor to work towards it. For this purpose, we will also further develop our sensors to produce more detailed readings that are reliable in different scenarios.

VI. Conclusion

This work shows the immense importance of evaluating MC testbeds for the internet of bio-nano things in blood. In the collected results, we see that the added complexity of the transmission in blood can offer new possibilities to improve communication in future medical applications. With the presented mathematical model, we provide a first theoretical description of MC in blood. To enable theoretical evaluations of the same, we presented a mathematical model to describe the CIR. It accurately describes the sensor behavior observed for blood and SPION movement. Although this work allows only for a first assessment and no generalization, it is an important first step for the transfer of simplified theoretical models to more complex behavior.

In future work, we will analyze the impact of different background flow fluids on communication performance in realistic in-body MC. At the same time, we will extend the evaluation of our testbed in blood to different blood characteristics and more complex networks. We will study the influence of pulsatile flow and different tubing materials on the channel response and use the discovered CIR characteristics to improve MC in blood.

References

[1] I. F. Akyildiz, M. Pierobon, S. Balasubramaniam, and Y. Koucheryavy, "The Internet of Bio-Nano Things," *IEEE Commun. Mag.*, vol. 53, no. 3, pp. 32–40, Mar. 2015.

[2] L. Brand, M. Garkisch, S. Lotter, M. Schäfer, A. Burkovski, H. Sticht, K. Castiglione, and R. Schober, "Media Modulation Based Molecular Communication," *IEEE Trans. Commun.*, vol. 70, no. 11, pp. 7207–7223, Nov. 2022.

[3] A. Wietfeld, S. Schmidt, and W. Kellerer, "Evaluation of a Multi-Molecule Molecular Communication Testbed Based on Spectral Sensing," in *IEEE GLOBECOM 2024*, Cape Town, South Africa, Dec. 2024.

[4] V. Jamali, A. Ahmadzadeh, W. Wicke, A. Noel, and R. Schober, "Channel Modeling for Diffusive Molecular Communication - A Tutorial Review," *Proc. IEEE*, vol. 107, no. 7, pp. 1256–1301, Jul. 2019.

[5] W. Wicke, T. Schwering, A. Ahmadzadeh, V. Jamali, A. Noel, and R. Schober, "Modeling Duct Flow for Molecular Communication," in *IEEE GLOBECOM 2018*, Abu Dhabi, United Arab Emirates, Dec. 2018, pp. 206–212.

[6] P. Hofmann, J. A. Cabrera, R. Bassoli, M. Reisslein, and F. H. P. Fitzek, "Coding in Diffusion-Based Molecular Nanonetworks: A Comprehensive Survey," *IEEE Access*, vol. 11, pp. 16 411–16 465, 2023.

[7] M. Kuscu, E. Dinc, B. A. Bilgin, H. Ramezani, and O. B. Akan, "Transmitter and Receiver Architectures for Molecular Communications: A Survey on Physical Design With Modulation, Coding, and Detection Techniques," *Proc. IEEE*, vol. 107, no. 7, pp. 1302–1341, Jul. 2019.

[8] V. Jamali, A. Ahmadzadeh, and R. Schober, "Symbol Synchronization for Diffusion-Based Molecular Communications," *IEEE Trans. on Nanobiosci.*, vol. 16, no. 8, pp. 873–887, Dec. 2017.

[9] L. Y. Debus, P. Hofmann, J. Torres Gómez, and F. Dressler, "Synchronized Relaying in Molecular Communication: An AI-based Approach using a Mobile Testbed Setup," *IEEE Trans. Mol. Biol. Multi-Scale Commun.*, vol. 10, no. 3, pp. 470–475, Sep. 2024.

[10] L. Huang, F. Liu, and L. Lin, "Molecular Communication Systems in Cylindrical Channels With Non-Newtonian Fluid Flows in IoBNT," *IEEE Internet Things J.*, vol. 11, no. 16, pp. 27 085–27 098, Aug. 2024.

[11] T.-R. Lee, M. Choi, A. M. Kopacz, S.-H. Yun, W. K. Liu, and P. Decuzzi, "On the near-wall accumulation of injectable particles in the microcirculation: smaller is not better," *Sci. Rep.*, vol. 3, no. 1, Jun. 2013.

[12] G. Yue, Q. Liu, and K. Yang, "Bio-Internet of Things Through Micro-Circulation Network: A Molecular Communication Channel Modeling," *IEEE Internet Things J.*, Jun. 2024.

[13] M. Bartunik, G. Fischer, and J. Kirchner, "The Development of a Biocompatible Testbed for Molecular Communication with Magnetic Nanoparticles," *IEEE Trans. Mol. Biol. Multi-Scale Commun.*, 2023.

[14] W. Wahood, S. Ghozy, A. Al-Abdulghani, and D. F. Kallmes, "Radial Artery Diameter: a Comprehensive Systematic Review of Anatomy," *J. of NeuroInterventional Surgery*, vol. 14, no. 12, pp. 1274–1278, 2022.

[15] S. Schneider, "Entwicklung einer Methode für die belastungsarme nichtinvasive Langzeitmessung des Blutdrucks," PhD Thesis, Technische Universität Berlin, Berlin, Germany, Aug. 2014.

[16] M. Bartunik, S. Faghih-Naini, T. Maiwald, and J. Kirchner, "Planar Coils for Detection of Magnetic Nanoparticles in a Testbed for Molecular Communication," in *ACM NANOCOM 2022*, Barcelona, Spain: ACM, Oct. 2022.

[17] C. Janko, J. Zaloga, M. Pöttler, S. Dürr, D. Eberbeck, R. Tietze, S. Lyer, and C. Alexiou, "Strategies to Optimize the Biocompatibility of Iron Oxide Nanoparticles – "SPIONs Safe by Design"," *JMMM*, vol. 431, pp. 281–284, Jun. 2017.

[18] P. Ecker, A. Sparer, B. Lukitsch, M. Elenkov, M. Seltenhammer, R. Crevenna, M. Gföhler, M. Harasek, and U. Windberger, "Animal Blood in Translational Research: How to Adjust Animal Blood Viscosity to the Human Standard," *Physiol. Rep.*, vol. 9, no. 10, May 2021.

[19] H. Unterweger, J. Kirchner, W. Wicke, A. Ahmadzadeh, D. Ahmed, V. Jamali, C. Alexiou, G. Fischer, and R. Schober, "Experimental Molecular Communication Testbed Based on Magnetic Nanoparticles in Duct Flow," in *IEEE SPAWC 2018*, Kalamata, Greece, Jun. 2018, pp. 1–5.

[20] F. M. White, *Fluid Mechanics* (Mcgraw-Hill series in mechanical engineering). McGraw-Hill, 2016, p. 773.

Lisa Y. Debus (Student Member, IEEE) received her B.Sc. in Computer Engineering from TU Berlin in 2022 and completed the consecutive M.Sc. in 2024. She is currently pursuing her Ph.D. degree with the Telecommunication Networks Group, Department of Telecommunication Systems, Technical University of Berlin, Berlin. Her research interests include Molecular Communication, the Internet of Bio-Nano Things, and Semantic Communication.

Mario J. Wilhelm is currently pursuing his bachelor's degree in Engineering Science at Technical University Berlin (TUB). He wrote his bachelor's thesis on this project at the Institute of Computer-assisted Cardiovascular Medicine (ICM) at Charité - Universitätsmedizin Berlin, where he is currently employed as a student assistant.

Henri Wolff obtained his M.Sc. in Engineering Science from TU Berlin in 2025 and is currently pursuing a Ph.D. in the Biofluid Mechanics Laboratory at Charité – Universitätsmedizin Berlin. He has been associated with the laboratory since 2021, following the completion of his B.Sc. in Engineering Science at TU Berlin, and has since contributed to research on the modeling of blood damage induced by blood-contacting medical devices. His work primarily focuses on the application of numerical methods to address problems in medical engineering.

Luiz C. P. Wille (Student Member, IEEE) received the B.Sc. degree in electrical engineering and the M.Sc. degree in biomedical engineering from the Technical University Chemnitz, Germany, in 2021 and 2024, respectively. In 2024, he joined the Institute for Smart Electronics and Systems, Friedrich-Alexander-Universität Erlangen-Nürnberg (FAU), formerly known as Institute for Electronics Engineering. His research interests include (medical) electronics, system modeling and numerical simulation, and the application of magnetic drug targeting.

Tim Rese received his B.Sc. in Engineering Science from the Technical University of Berlin in 2017 and completed the consecutive M.Sc. in 2021. He Worked from 2020 in the Biofluid Mechanics Laboratory , Institute of Computer-assisted Cardiovascular Medicine of the Charité Universitätsmedizin Berlin and is currently finishing his Ph.D degree. His research interests focus on the development of ventricular assist devices and total artificial hearts, aerosol research, and the Internet of Bio-Nano Things.

Michael Lommel is the group leader of the Biofluid Mechanics Laboratory at Charité – Universitaetsmedizin Berlin. He received his diploma in mechanical and biomedical engineering in 2012 and his PhD in 2025 from TU Berlin. His research focuses on hemorheology and the experimental investigation of blood damage caused by blood-carrying devices. He has worked for several years on developing new blood pump concepts, focusing on optimised blood flow to reduce complications caused by damage to various blood components. He is part of the leadership team of the transdisciplinary Global Resist project, which deals with forecasting antibiotic resistance evolution. He is also part of the SPARK Innovation Team at the Berlin Institute of Health, focusing on the transfer of research discoveries into clinical practice.

Jens Kirchner (Senior Member, IEEE) received the Diploma and Ph.D. degrees in physics as well as the Ph.D degree in philosophy from Friedrich-Alexander-Universität Erlangen-Nürnberg (FAU), in 2004, 2008 and 2016, respectively. From 2008 to 2015, he worked for Biotronik SE and Co. KG in research and development of implantable cardiac sensors. From 2015 to 2023, he headed the research group for Medical Electronics and Multiphysical Systems at the Institute for Electronics Engineering, FAU. Since 2023, he has been full professor for Electronics in Medical Engineering with the Department of Information Technology at University of Applied Sciences and Arts Dortmund.

Dr. Dr. Kirchner is Senior Member of the IEEE as well as member of the Association for Computing Machinery (ACM), the German Society for Biomedical Engineering within VDE (VDE DGBMT). He has been reviewer for journals and conferences of these associations and has authored a textbook on scientific working techniques published by Springer.

The research of Dr. Dr. Kirchner is focused on sensing and magnetic targeting of nanoparticles for use in molecular communication and cancer therapy. Further research interests include wearable sensors for chronic disease monitoring and the power supply for such sensors by use of energy harvesting and inductive transcutaneous power transfer. Furthermore, he is interested in the ethical aspects of these research topics.

Falko Dressler (Fellow, IEEE) is full professor and Chair for Telecommunication Networks at the School of Electrical Engineering and Computer Science, TU Berlin. He received his M.Sc. and Ph.D. degrees from the Dept. of Computer Science, University of Erlangen in 1998 and 2003, respectively.

Dr. Dressler has been associate editor-in-chief for IEEE Trans. on Network Science and Engineering, IEEE Trans. on Mobile Computing and Elsevier Computer Communications as well as an editor for journals such as IEEE/ACM Trans. on Networking, Elsevier Ad Hoc Networks, and Elsevier Nano Communication Networks. He has been chairing conferences such as IEEE INFOCOM, ACM MobiSys, ACM MobiHoc, IEEE VNC, IEEE GLOBECOM. He authored the textbooks Self-Organization in Sensor and Actor Networks published by Wiley & Sons and Vehicular Networking published by Cambridge University Press. He has been an IEEE Distinguished Lecturer and an ACM Distinguished Speaker.

Dr. Dressler is an IEEE Fellow, an ACM Fellow, and an AAIA Fellow. He is a member of the German National Academy of Science and Engineering (acatech). He has been serving on the IEEE COMSOC Conference Council and the ACM SIGMOBILE Executive Committee. His research objectives include next generation wireless communication systems in combination with distributed machine learning and edge computing for improved resiliency. Application domains include the internet of things, cyber-physical systems, and the internet of bio-nano-things.